ARTICLE

BIOTECHNOLOGY and BIOENGINEERING

Effects of Glucose and Insulin on HepG2-C3A Cell Metabolism

Vidya V. Iyer,[1] Hong Yang,[1] Marianthi G. Ierapetritou,[1] Charles M. Roth[1,2]

[1]Department of Chemical and Biochemical Engineering, The State University of New Jersey, Piscataway, New Jersey 08854; telephone: 732-445-4500x6205; fax: 732-445-3753; e-mail: cmroth@rci.rutgers.edu

[2]Department of Biomedical Engineering, Rutgers, The State University of New Jersey, Piscataway, New Jersey

Received 16 January 2010; revision received 31 March 2010; accepted 6 May 2010

Published online 18 May 2010 in Wiley Online Library (wileyonlinelibrary.com). DOI 10.1002/bit.22799

ABSTRACT: HepG2, hepatocellular carcinoma cells, are used in drug toxicity studies and have also been explored for bioartificial livers. For these applications, the cells are under variable levels of nutrients and hormones, the effects of which on metabolism are poorly understood. In this study, HepG2-C3A cells were cultured under varying levels of glucose (high, low, and glucose-free) and insulin (without and with physiological levels of insulin) for 5 days. Cell growth was found to be comparable between high and low glucose media and lowest for glucose-free medium. Several features of central metabolism were affected profoundly by the medium glucose levels. Glucose consumption was greater for low glucose medium compared to high glucose medium, consistent with known glucose feedback regulation mechanisms. Urea productivity was highest in glucose-free medium. Further, it was seen that lactate acted as an alternative carbon source in the absence of glucose, whereas it acted as a sink for the high and low glucose media. Using a metabolic network flexibility analysis (MNFA) framework with stoichiometric and thermodynamic constraints, intracellular fluxes under varying levels of glucose and insulin were evaluated. The analysis indicates that urea production in HepG2-C3A cells arises via the arginase II pathway rather than from ammonia detoxification. Further, involvement of the putrescine metabolism with glutamine metabolism caused higher urea production in glucose-free medium consistent with higher glutamine uptake. MNFA indicated that in high and low glucose media, glycolysis, glutaminolysis, and oxidative phosphorylation were the main sources of energy (NADH, NADPH, and ATP). In the glucose-free medium, due to very low glycolytic flux, higher malate to pyruvate glutaminolytic flux and TCA cycle contributed more significantly to energy metabolism. The presence of insulin lowered glycerol uptake and corresponding fluxes involved in lipid metabolism for all glucose levels but otherwise exerted negligible effect on metabolism. HepG2-C3A cells thus show distinct differences from primary hepatocytes in terms of energy metabolism and urea production. This knowledge can be used to design media supplements and metabolically engineer cells to restore necessary hepatic functions to HepG2-C3A cells for a range of applications.

Biotechnol. Bioeng. 2010;107: 347–356.

KEYWORDS: metabolic network flexibility analysis; hepatocellular carcinoma; glutaminolysis; urea production; energy metabolism; hexokinase II

Introduction

HepG2, hepatocellular carcinoma cells, are easily maintained and expanded in culture and have been shown to express a wide range of liver-specific functions. As such, HepG2 cells can be used for basic studies of hepatocyte cellular physiology such as response to inflammatory stimuli (Roth et al., 2001) and as metabolically relevant models for in vitro toxicology studies (Plant, 2004; Wilkening et al., 2003). They have also been evaluated as the cell source for bioartificial livers (Allen et al., 2001; Park and Lee, 2005). Although the molecular expression of HepG2 cells and biological phenotypes have been characterized extensively (Javitt, 1990; Porat et al., 1995; Ranheim et al., 2006), relatively little quantitative data exists regarding metabolic fluxes in response to simple medium perturbations. In a bioreactor, the levels of nutrients and hormones will vary with space and/or time depending on the configuration chosen (Tilles et al., 2002). The design and operation of bioreactors employing HepG2 cells would be aided by improved understanding of their response to varying nutrient and metabolite levels.

Correspondence to: Charles M. Roth

Contract grant sponsor: NSF QSB CBET Program
Contract grant number: BES-0424968
Contract grant sponsor: NSF Metabolic Engineering
Contract grant number: BES-0519563
Contract grant sponsor: USEPA-funded Environmental Bioinformatics and Computational Toxicology Center
Contract grant number: GAD R 832721-010

Additional Supporting Information may be found in the online version of this article.

HepG2 cells, being cancer cells of the liver, exhibit both hepatocyte and tumor cell characteristics. Glycolysis or gluconeogenesis is the starting point of carbon flow into or out of primary metabolism in hepatocytes and hence directly impacts the regulation of various pathways such as urea production, lipid metabolism and glutamine metabolism. Glycolysis, in conjunction with glutaminolysis, is also the main source of energy in tumor cells compared to oxidative phosphorylation (Colowick, 1961; DeBerardinis et al., 2007; Moreadith and Lehninger, 1984; Moreno-Sanchez et al., 2007). Hence, we explored the effects of varying levels of glucose on the interactions of primary metabolic pathways and energy metabolism. Further, insulin, an anabolic hormone, helps regulate lipid metabolism and gluconeogenesis in primary hepatocytes (Chan et al., 2002), and its level may also be an important parameter in the medium in conjunction with glucose.

Flux balance analysis (FBA) is an important tool for quantification of intracellular fluxes in a metabolic network using extracellular measurements, metabolite balances and an objective function such as minimization of the error between experimental and calculated fluxes (Stephanopoulos et al., 1998; Varma and Palsson, 1994). A related approach called metabolic network flexibility analysis (MNFA) involves minimization and maximization of all the fluxes in a constraint-based optimization framework, thereby calculating a range for each unmeasured intracellular flux (Llaneras and Picó, 2007a,b; Yang et al., submitted). In single-cell organisms with clearly defined metabolic objectives, metabolic fluxes are useful for comparing genetic or environmental variants as well as for suggesting possible targets of genetic modification (Nielsen, 1998). Metabolic fluxes have been employed previously to understand effects of burn injury on liver function (Lee et al., 2003), as well as those of hormone supplementation and plasma exposure on cultured hepatocytes (Chan et al., 2003b). More recently, a study on HepG2 cells treated with free fatty acids employed intracellular flux analysis to reveal lower glutathione synthesis due to reduced cysteine uptake (Srivastava and Chan, 2008).

In this study, HepG2-C3A cells were cultured in vitro under varying levels of glucose and insulin for 5 days. A number of metabolites were measured, including glucose, lactate, urea, amino acids, glycerol, fatty acids, cholesterol and acetoacetate. MNFA was employed to calculate the intracellular fluxes using extracellular measurements and system constraints to elucidate the changes in metabolism with varying treatments.

Materials and Methods

Cell Culture

HepG2-C3A cells (ATCC, Manassas, VA) were maintained in T75 plates in ATCC-recommended minimal essential media containing 1 mg/mL glucose. Around passage 7, cells were harvested and seeded in 6 well plates at 0.4 million cells/mL. The following day, media were changed and each well of cells was treated with one of six different medium compositions. The media primarily consisted of DMEM glucose-free (Invitrogen, Carlsbad, CA) supplemented with 10% FBS (Invitrogen), 1% sodium pyruvate (Invitrogen), 2% Penicillin–Streptomycin (Invitrogen) with three varying levels of glucose (Fisher Scientific, Pittsburgh, PA): high glucose (3 mg/mL), low glucose (1 mg/mL) or glucose-free (0 mg/mL). Further, cells were cultured either without insulin or with physiological levels of insulin, 50 μU/mL. All treatments were carried out in triplicate. The media were changed every 24 h for 5 days, and supernatants were collected and stored in −80°C freezer for further analysis. Cell counts were also determined every 24 h for all six treatments using the ethidium homodimer assay.

Cell Growth

Cells were quantified by first killing them in 75% methanol for 30 min and then staining with ethidium homodimer (Sigma, St. Louis, MO). After washing the plate with PBS twice, 1 mL of 0.2 mM ethidium homodimer solution was added to each well, and the plates were wrapped to protect them from light. The plates were incubated at room temperature for 45 min after which the fluorescence was measured at 530 nm excitation and 645 nm emission wavelengths. Using a standard curve prepared separately, the total number of cells was calculated for each treatment for all 5 days.

Extracellular Metabolite Measurements

The following metabolites were quantified using commercial kits: glucose, triglycerides (TG) and glycerol (Sigma), lactate (Trinity Biotech, Berkeley Heights, NJ); β-hydroxybutyrate and urea (Fisher Scientific); cholesterol (Bioassay Systems, Hayward, CA); and free fatty acids (Roche Diagnostics, Indianapolis, IN). Acetoacetate was measured using the protocol adapted by Chan et al. (2003a). Albumin production was measured using the ELISA assay and was found to be negligible. The levels of 19 amino acids (Asp, Glu, Gly, Arg, Thr, Ala, Pro, Tyr, Val, Met, Lys, Ile, Leu, Phe, Ser, Cys, Orn, Asn, and His) were measured using HPLC and the AccqTag method (Waters, Milford, MA), whereas glutamine was quantified using a commercial kit from Sigma.

Metabolic Network Flexibility Analysis

The metabolic network constructed for the central metabolism of HepG2-C3A cells is shown in Fig. S1 (supplementary material). The network consisted of glycolysis, pentose phosphate pathway, lactate production,

tricarboxylic acid (TCA) cycle, urea production, lipid metabolism and amino acid metabolism reactions. The reaction of methionine degradation to cysteine was omitted due to the absence of the corresponding enzyme in HepG2 cells (Srivastava and Chan, 2008). The malate to pyruvate reaction was added to complete the glutaminolytic pathway prevalent in tumor cells (Wise et al., 2008). For urea production, the urea cycle found in hepatocytes was retained in the network. Urea production through the arginase II pathway and subsequent putrescine metabolism was also included for the HepG2-C3A metabolic network as seen in recent literature (Mavri-Damelin et al., 2008; Srivastava and Chan, 2008). In total, the network consists of 74 reactions and 44 metabolites (Tables S1 and S2). Further, 27 extracellular fluxes were measured (Table S3) leading to an underdetermined system of equations.

Fluxes were evaluated using a modification of the flux spectrum approach (Llaneras and Picó, 2007b; Wiback et al., 2004) that we term metabolic network flexibility analysis (MNFA). This procedure involves solving, separately, minimization and maximization linear programming problems for each of the unmeasured fluxes, thereby calculating a flux range for each unmeasured flux subject to system constraints (Yang et al., submitted).

$$\begin{aligned} &\underset{j\in E}{\text{Max/Min}} \quad v_j \\ &s.t. \qquad \sum_j^N S_{ij}v_j = 0 \qquad i \in M \\ &\qquad\quad v_j^{\min} < v_j < v_j^{\max} \quad j \in K \\ &\qquad\quad \sum_j^N \Delta G_p^0 v_j \le 0 \qquad p \in P \end{aligned} \tag{1}$$

where v_j is the reaction rate of reaction j, S_{ij} is the stoichiometric coefficient of metabolite i in reaction j. The fluxes $v_j^{\min}$ and $v_j^{\max}$ are the lower and upper bound of constrained reactions, respectively, M is the set of metabolites, N is the total number of reactions involved in the hepatic network, K is the set of constrained reactions (based on measurements and/or irreversibility), P is the number of elementary pathways computed by generating extreme vectors of pointed convex cones (Schuster et al., 2000, 2002), implemented in Matlab software *Fluxanalyzer* (Klamt et al., 2003) and E is the set of unknown reactions. The matrix of elementary pathways weighted by Gibbs energy of reactions is denoted by ΔG_{p} ($P \times N$ dimension).

The main assumptions for the development of the MNFA model are as follows: (1) The internal metabolites are assumed to be maintained at pseudo-steady state, which means their rate of change is small compared to their turnover; (2) The constraints for irreversible reactions, $v_j \ge 0$, are imposed based on the information from KEGG (Kanehisa and Goto, 2000); (3) The value of each measured flux is constrained by an interval $[v_{\min}, v_{\max}]$ corresponding to its average and standard derivation of triplicate measurements; (4) Pathway energy balance (PEB) constraints using standard Gibbs energies of the metabolites (Mavrovouniotis, 1991) are added to reduce and more accurately describe the feasible range of intracellular fluxes (Nolan et al., 2006; Yang et al., submitted).

Considerations for the pseudo-steady state assumption include the growth of the cells and the resulting changes in extracellular metabolite concentrations. It has recently been demonstrated in HepG2-C3A cells that the fluxes are considerably higher than the actual changes in the intracellular metabolite concentration, thereby providing support for the validity of the pseudo-steady-state approximation (Srivastava and Chan, 2008). In this work, depletion of glucose is observed in the low glucose experimental condition at days 4 and 5; however, the resulting flux changes are relatively small. Nonetheless, the flux should be considered as an average over each 24-h period. Partly due to this issue, we focus our detailed metabolic analysis on day 3 metabolic flux data, where the pseudo-steady-state approximation is likely the most accurate.

Statistical analysis among treatments was performed using analysis of variance (ANOVA) followed by Tukey's studentized range test, performed with SAS software (SAS Institute, Inc., Cary, NC). Two samples did not survive processing on the last day; for these, missing value estimation was performed based on the mean and global variance. MNFA was performed for days 2, 3, and 5 data for all the treatments and the metabolic fluxes are listed in the supplementary material (Tables S4–S6). We found large standard deviations in the extracellular measurements for day 1 for all treatments. It is most likely that the cells needed to adapt when switched from the ATCC-recommended minimal essential medium with 1 mg/mL of glucose to DMEM with varying levels of glucose and insulin. Hence, we did not perform MNFA of day 1. The trends between days 3 and 5 were always linear and hence we did not perform MNFA of day 4.

Results

HepG2-C3A cells were cultured for 5 days under three different levels of glucose—3 mg/mL (high), 1 mg/mL (low) and 0 mg/mL (glucose-free)—each with and without physiological levels of insulin, for a total of six growth conditions. Cell growth and metabolism were measured throughout the time frame. We observed that insulin affected very few fluxes (see later section) and thus, except where noted, only the data without exogenous insulin are reported. Complete extracellular measurements and intracellular flux calculations are listed in the supplementary material (Tables S4–S6) for each of the six conditions.

Experimental Measurements

HepG2-C3A cell growth was sustained regardless of glucose level, with the highest growth rate exhibited by cells in low

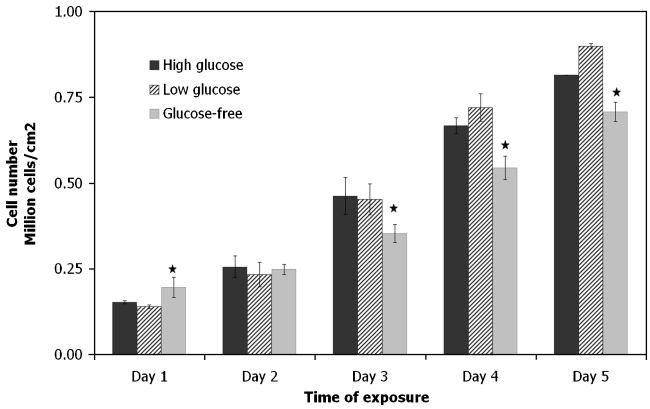

Figure 1. Cell growth exhibits an optimum with respect to glucose concentration in the medium. Total number of cells was counted daily using the ethidium homodimer assay. High glucose (3 mg/mL), low glucose (1 mg/mL) and glucose-free (0 mg/mL) represent varying levels of glucose in the growth medium, which was changed daily. * represents statistically significantly different ($P < 0.05$) from low glucose medium.

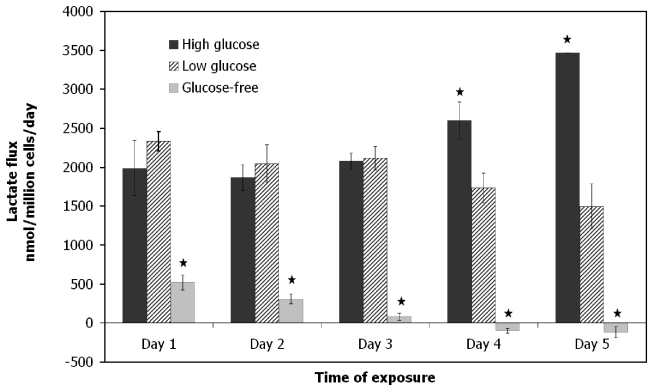

Figure 3. Lactate production flux increases in high glucose medium, and lactate is consumed after several days of culture in glucose-free medium. Fluxes were calculated based on the change in media lactate concentrations on successive days, normalized to cell number. High glucose (3 mg/mL), low glucose (1 mg/mL) and glucose-free (0 mg/mL) represent varying levels of glucose respectively. * represents statistically significantly different ($P < 0.05$) from low glucose medium.

glucose and high glucose media and the lowest growth rate by those in glucose-free medium (Fig. 1). HepG2-C3A cells consumed glucose under all conditions, consistent with a glycolytic phenotype. The glucose consumption flux decreased from day 1 through day 5 for both high glucose and glucose-free media (Fig. 2). In the "glucose-free" medium, there is a very small amount of glucose (<0.23 mM) present in the fetal bovine serum, which contributes to the negligible glucose consumption flux. For low glucose medium, the glucose consumption flux was steady for the first 3 days and then decreased from days 3 to 5 (Fig. 2). The decrease in the glucose consumption flux at days 4 and 5 for low glucose medium can be explained by the lack of availability of glucose in the medium. As seen in Figure S2, the glucose concentration in the supernatant drops considerably from days 1 to 5 for low glucose medium, associated with the increase in cell number over the same time period, with essentially all of the available glucose consumed on days 4 and 5.

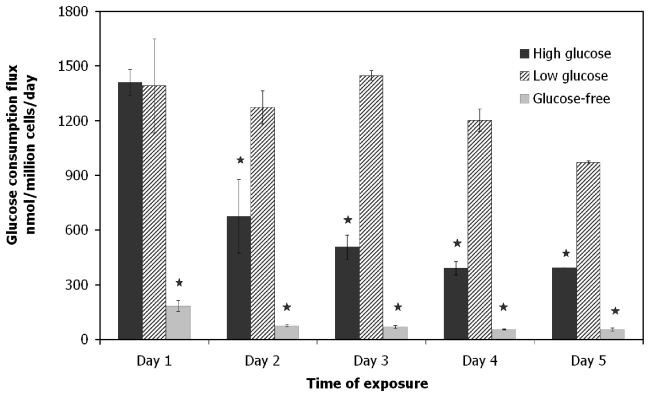

Figure 2. Glucose consumption flux is maintained at high levels for low glucose medium. Fluxes were calculated based on the change in media glucose concentrations on successive days, normalized to cell number. High glucose (3 mg/mL), low glucose (1 mg/mL), and glucose-free (0 mg/mL) represent varying levels of glucose respectively. * represents statistically significantly different ($P < 0.05$) from low glucose medium.

We observed that the glucose consumption flux was always higher for low glucose medium than for high glucose medium, except on day 1 where they were comparable (Fig. 2). We also observed that the glucose concentration in the supernatant for high glucose medium (Fig. S2 in supplementary material), remains level from days 1 to 5. Since the hexokinase enzyme (which catalyzes the conversion of glucose to G6P in the first step of the glycolytic pathway) is feedback inhibited by high concentrations of G6P (Marin-Herandez et al., 2006), it is feasible that the glucose consumption is controlled by the high concentration of glucose in the media.

It is well known that tumor cells produce lactate in response to an increased glycolytic activity (Moreno-Sanchez et al., 2007; Warburg, 1956). For high glucose medium, lactate production increased from days 1 to 5, whereas it did not vary with time for low glucose medium (Fig. 3). Lactate thus acted as a sink in the medium containing high glucose. The lactate production was lowest for glucose-free medium (Fig. 3), decreasing from days 1 to 3 followed by a switch to lactate consumption, which is possible due to the small amount of lactate in the media from the fetal bovine serum. Thus, lactate acted as an alternative source of carbon for cells cultured in glucose-free media.

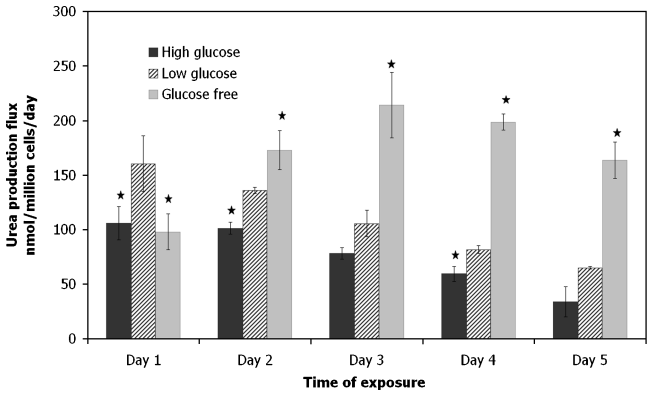

Figure 4. Urea production flux is increased in glucose-free medium. Fluxes were calculated based on the change in media urea concentrations on successive days, normalized to cell number. High glucose (3 mg/mL), low glucose (1 mg/mL) and glucose-free (0 mg/mL) represent varying levels of glucose respectively. * represents statistically significantly different ($P < 0.05$) from low glucose medium.

Urea production is an important flux in liver cells as a standard marker of nitrogen metabolism. Urea production decreased from days 1 to 5 for low and high glucose media, with low glucose medium consistently producing more urea (Fig. 4). For glucose-free medium in contrast, the urea production flux was initially moderate but increased to day 3 and remained elevated compared to the other conditions for the duration of the experiment.

Metabolic Network Flexibility Analysis

The metabolic network constructed for the central metabolism of HepG2-C3A cells is shown in Figure S1 (supplementary material). Metabolic network flexibility analysis (MNFA) involves the quantification of intracellular fluxes in a biological system, using reaction stoichiometry, thermodynamic constraints and extracellular measurements in an optimization framework that involves calculation of a feasible range for each unmeasured flux (Llaneras and Picó, 2007a,b; Yang et al., submitted).

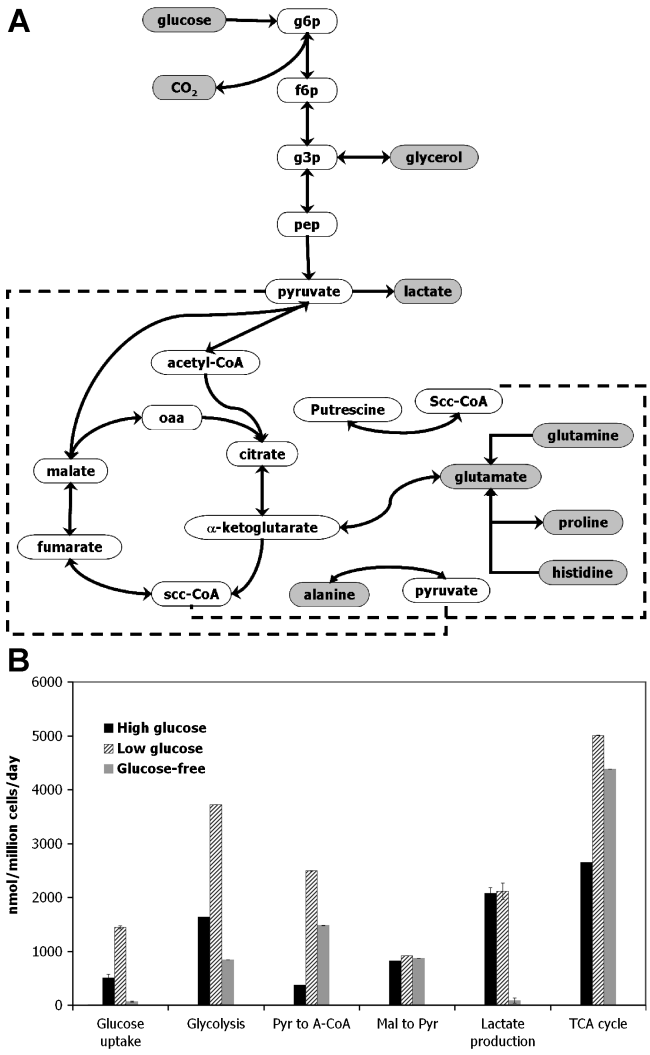

Figure 5. **A**: Simplified pathway representing glucose utilization and glutaminolysis. Metabolites in gray ovals signify extracellular metabolites. For the sake of clarity, dashed lines link metabolites that are connected and occur in different parts of the pathway. **B**: Metabolic flux range (calculated by MNFA) for reactions corresponding to glucose utilization for day 3 for without insulin treatment. Calculated flux ranges were tight for all the treatments and are represented as a bar graph. Glucose uptake and lactate production are measured extracellular fluxes. High glucose (3 mg/mL), low glucose (1 mg/mL) and glucose-free (0 mg/mL) represent varying levels of glucose respectively.

Glycolysis, Glutaminolysis, and Energy Metabolism

Glycolysis provides a source of carbon into central metabolism and is a major primary source of energy in tumor cells (Colowick, 1961; Marin-Herandez et al., 2006). Lactate production from pyruvate is an important characteristic of tumor cells with high glycolytic activity (Moreno-Sanchez et al., 2007). For day 3, lactate production is comparable between high glucose and low glucose media and is very low for glucose-free medium (Fig. 5). The main reactions contributing to the pyruvate pool are glycolysis and the anaplerotic reaction of malate to pyruvate. Glucose uptake is considerably higher in low glucose medium compared to high glucose medium, presumably because of feedback inhibition of the hexokinase enzyme by high concentrations of glucose-6-phosphate (Marin-Herandez et al., 2006). Consequently, glycolytic flux is higher in low glucose medium compared to high glucose medium. As expected, cells in glucose-free medium exhibit very low glycolysis. In contrast, the malate to pyruvate flux is similar among varying levels of glucose and is fed by glutaminolytic reactions that involve incorporation of glutamine to replenish metabolites in the TCA cycle (Fig. 5).

Some of the important energy producing reactions in tumor cells are glycolysis (NADH and ATP production),

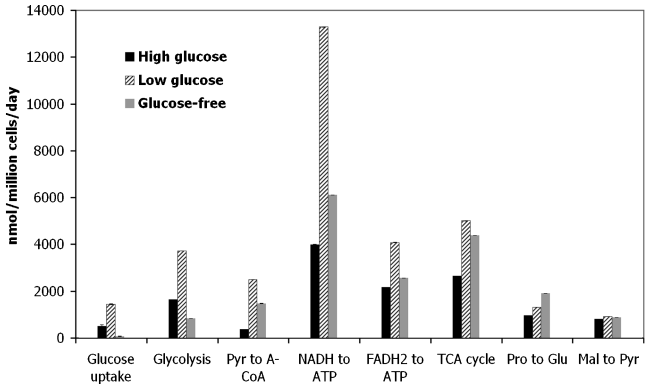

Figure 6. Metabolic flux range (calculated by MNFA) for reactions corresponding to energy metabolism on day 3 for without insulin treatment. Calculated flux ranges were tight for all the treatments and are represented as a bar graph. Glucose uptake is a measured extracellular flux. High glucose (3 mg/mL), low glucose (1 mg/mL) and glucose-free (0 mg/mL) represent varying levels of glucose respectively.

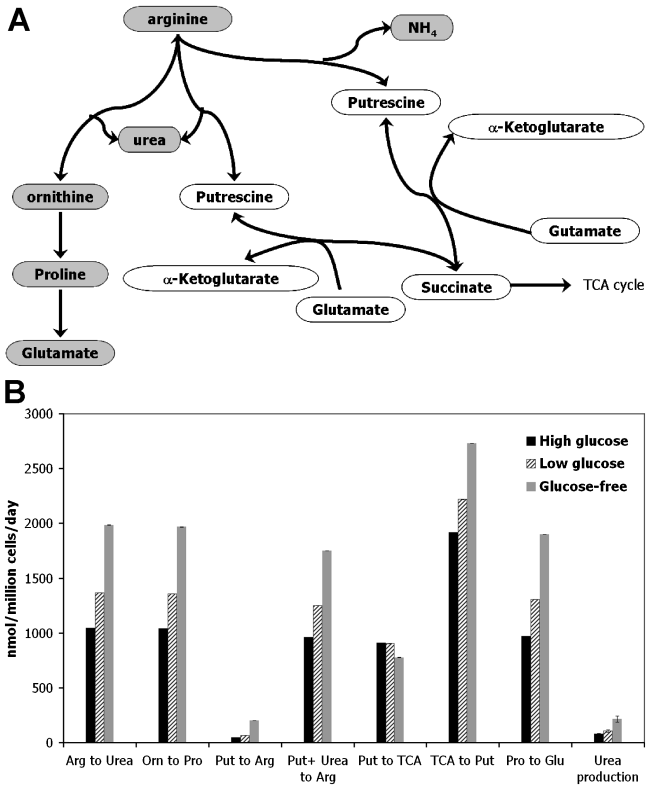

Figure 7. **A**: Simplified pathway representing urea production in HepG2-C3A cells. Metabolites in gray ovals signify extracellular metabolites. **B**: Metabolic flux range (calculated by MNFA) for reactions corresponding to urea production on day 3 for without insulin treatment. Calculated flux ranges were tight for all the treatments and are represented as a bar graph. Arginine uptake and urea production are extracellular measurements. High glucose (3 mg/mL), low glucose (1 mg/mL) and glucose-free (0 mg/mL) represent varying levels of glucose respectively.

glutaminolysis (produces NADPH and NADH via TCA cycle), pyruvate oxidation (produces NADH), oxidative phosphorylation (produces ATP through the electron transport chain) and conversion of proline to glutamate (produces NADPH) in the urea synthesis pathway. Hepatocytes usually have electron transport chain (ETC) fluxes that are 20–30 times higher than glycolytic fluxes (Chan et al., 2003a). Comparatively, the contribution of electron transport chain (ETC) reactions (NADH/FADH2 to ATP) is modest in HepG2-C3A cells (Fig. 6). Only in the case of glucose-free medium, where the glycolytic flux is quite low, are the malate to pyruvate glutaminolytic flux, TCA cycle flux and proline to glutamate flux comparatively high.

Urea Production and Metabolism

Urea is produced in hepatocytes through a urea cycle that includes the important function of ammonia detoxification (Krebs and Henseleit, 1932). It has been shown recently that HepG2-C3A cells produce urea through a different pathway and do not detoxify ammonia (Mavri-Damelin et al., 2007, 2008). Thus, we utilized a metabolic network that includes the conventional urea cycle and the newly suggested pathways for urea production, including putrescine metabolism (Fig. 7A). For all three glucose treatments, MNFA indicated negligible fluxes through the ammonia detoxification steps of the conventional urea cycle (Table S5 in supplementary material, fluxes 41 and 42). Arginine uptake is low, and urea is produced through the arginase II pathway and also involves considerable activity through putrescine metabolism (Fig. 7B).

To understand the high extent of urea production in glucose-free medium, the reactions that are linked closely with urea production were investigated. Glutamine metabolism is directly associated with urea production, as putrescine metabolism involves the inter-conversion of glutamate and α-ketoglutarate (Fig. 7A). Putrescine metabolism also includes succinate production which links it to the TCA cycle. Thus, the high level of glutamine uptake in glucose-free medium can explain the highest urea production in glucose-free medium (Fig. S3).

Effects of Insulin

The presence of physiological levels of insulin affected primarily reactions involved in lipid metabolism. There was a considerably lower glycerol uptake for cells cultured with added insulin compared to without insulin for all three glucose treatments (Fig. 8). This directly impacted and caused a lower conversion of glycerol to G3P in the presence of insulin. The ketone body production, triglyceride production and fatty acid synthesis were also lowered but to a much lesser extent. It has been observed previously that preconditioning hepatocytes in physiological levels of

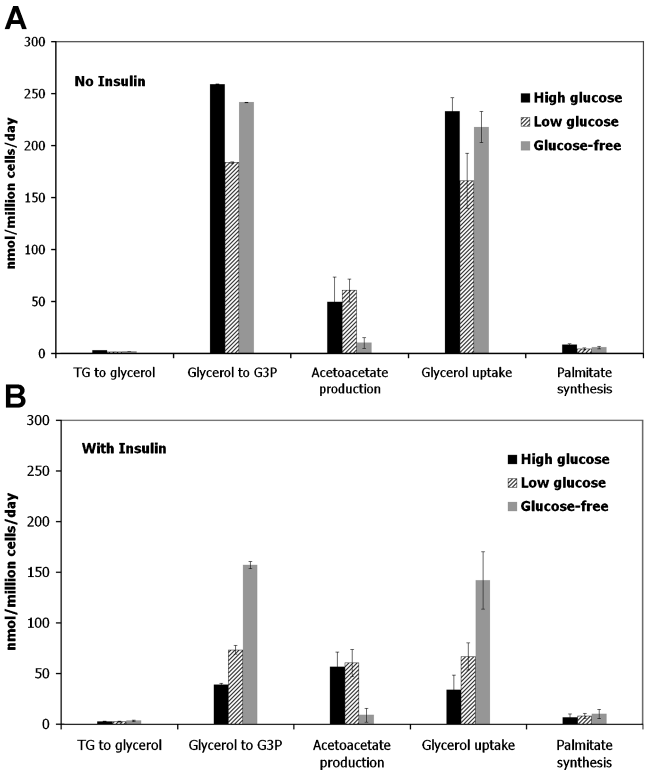

Figure 8. Metabolic flux range (calculated by MNFA) for reactions corresponding to lipid metabolism on day 3 for (**A**) No insulin treatment and (**B**) With insulin treatment. Calculated flux ranges were tight for all the treatments and are represented as a bar graph. Glycerol uptake and acetoacetate production are measured extracellular fluxes. High glucose (3 mg/mL), low glucose (1 mg/mL) and glucose-free (0 mg/mL) represent varying levels of glucose respectively.

insulin, as opposed to supraphysiological levels, lowered lipid accumulation (Chan et al., 2002, 2003a).

Temporal Variations in Fluxes Among Treatments

Overall, the calculated intracellular fluxes did not change dramatically with time, indicating that the MNFA calculation procedure is robust with respect to experimental variability manifest over multiple time points. Furthermore, comparisons among the glucose levels held for days 2 and 5 as well as for the day 3 presented in detail. An indication of the temporal variations is illustrated using glycolysis and its closely associated pathways. The limited availability of glucose for an increasing cell mass results in a systematic decline in glycolysis, pyruvate utilization and lactate production in low glucose and glucose-free media (Fig. 9). In fact, cells cultured in glucose-free media switch over to lactate consumption for day 5. Thus, lactate acts as an alternative carbon source in glucose-free medium. In high glucose medium, availability of glucose is not limited and thus the glycolytic flux is buffered. Nonetheless, lactate production is increased at

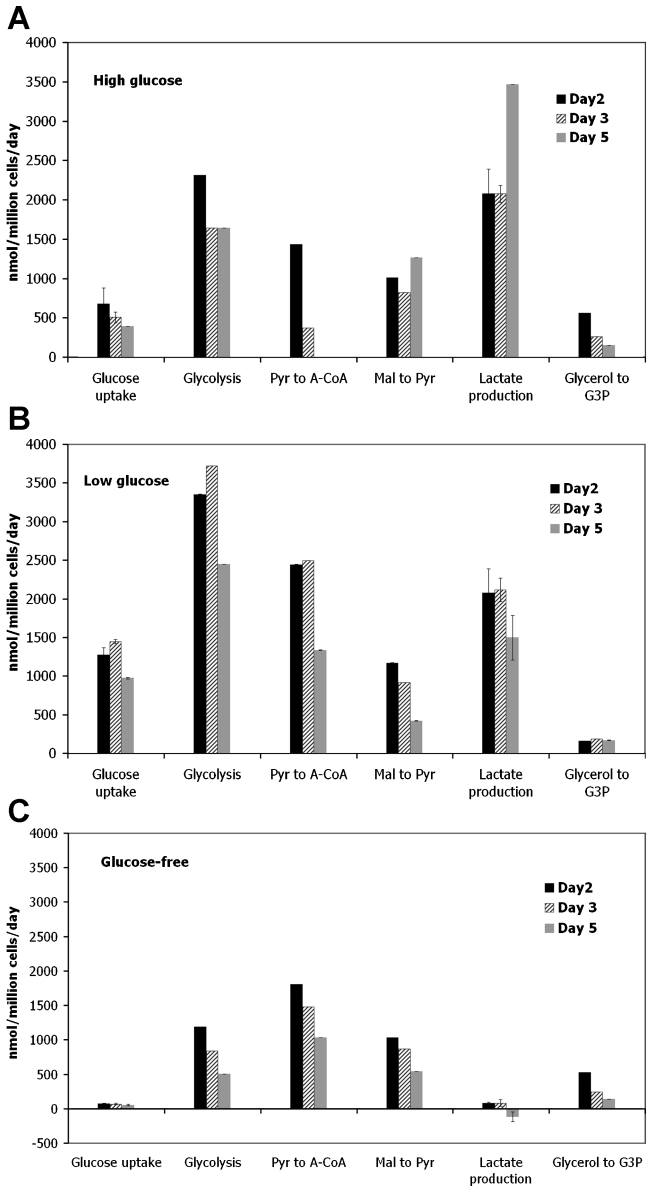

Figure 9. Metabolic flux range (calculated by MNFA) for reactions corresponding to glycolytic pathway on a temporal basis for without insulin treatment for (**A**) High glucose (3 mg/mL) (**B**) Low glucose (1 mg/mL) and (**C**) Glucose-free (0 mg/mL). Calculated flux ranges were tight for all the treatments and are represented as a bar graph. Glucose uptake and lactate production are extracellular measurements.

day 5 via increased pyruvate production originating in part from glutaminolysis.

Discussion

An underappreciated issue in using HepG2 cells concerns the extent to which the observable phenotypes are affected by the composition of the culture medium. Both glucose, a primary source of carbon in most cell culture media and insulin, an anabolic hormone, have direct impact on the

regulation of multiple pathways in central metabolism. Further, glycolysis is an important source of energy in tumor cells in addition to oxidative phosphorylation (Colowick, 1961; Moreno-Sanchez et al., 2007; Pedersen, 2007). In this study, HepG2-C3A cells were cultured in varying levels of glucose and insulin. Insulin is known to regulate glycolysis/gluconeogenesis, and an effect of insulin on glucose metabolism was expected. The differences in the measured fluxes were, however, less substantial than might be anticipated. With metabolic network flexibility analysis (MNFA), the origins of the observed differences with insulin were attributed to lipid metabolism (Fig. 8), similar to effects observed previously in hepatocyte culture (Barthel and Schmoll, 2003; Chan et al., 2002, 2003b).

Urea production is a marker of detoxification of ammonia in liver cells. Intracellular flux data revealed that the production of urea in HepG2-C3A cells is through the arginase II pathway and not through conventional detoxification of ammonia as found in primary hepatocytes (Fig. 7). Similar results were also observed in another flux analysis study (Srivastava and Chan, 2008) and also more directly through gene expression studies in HepG2-C3A cells (Mavri-Damelin et al., 2008). The absence of the important ammonia detoxification function potentially hinders the applicability of these cells in bioartificial livers. However, it was shown recently that transfection of HepG2 cells with cDNA constructs encoding ornithine transcarbamylase and arginase I restored the urea cycle (Mavri-Damelin et al., 2007). In our study, it was also observed that urea production was highest for glucose-free medium (Fig. 4). Glutamine acts as an alternative carbon source through the glutaminolytic pathway (DeBerardinis et al., 2007), and the uptake of glutamine is correspondingly higher in the glucose-free medium. Putrescine metabolism through the arginase II pathway involves the inter-conversion of glutamate and α-ketoglutarate (Fig. 7). Putrescine metabolism further includes succinate production, which links it to the TCA cycle. Thus, there is a direct association of glutamine with multiple pathways in primary metabolism, and glutamine uptake being highest in the glucose-free medium could explain the highest urea production in glucose-free medium (Fig. S3).

The energy production in primary hepatocytes is predominantly through oxidative phosphorylation (Chan et al., 2003a,b), whereas tumor cells have been shown to use glycolysis also for energy production (Colowick, 1961; Lopez-Rios et al., 2007; Mathupala et al., 2006). Glutaminolysis is the source of reductive co-factor (NADPH) in tumor cells and also replenishes the TCA cycle metabolites (DeBerardinis et al., 2007; Mazurek et al., 1999; Moreadith and Lehninger, 1984). We observed that in the high and low glucose media, glycolysis was one of the main sources of energy, glutaminolysis replenished TCA cycle metabolites, and oxidative phosphorylation was low (as compared to hepatocytes) (Fig. 6). The conversion of proline to glutamate, which produces NADPH, in the urea synthesis pathway was also lower for high and low glucose media compared to glucose-free medium. Thus, the lack of glucose in the glucose-free medium is compensated by the flexibility of the metabolic network, specifically via higher rates of glutaminolysis and of oxidative phosphorylation relative to glycolytic flux.

It has been well characterized that Glut1 is the main transporter of glucose in HepG2 cells (Mathupala et al., 2006; Takanaga et al., 2008). After entering into the cells, glucose is converted to glucose-6-phosphate (G6P) by the hexokinase II enzyme, expressed highly in most tumor cells (Mathupala et al., 2006; Pedersen et al., 2002), followed by subsequent metabolism of G6P in the glycolytic pathway. We observed that the glycolytic rate was, perhaps counter-intuitively, highest for low glucose medium despite availability of abundant glucose in the high glucose medium. The regulation of the glycolytic pathway has been found to be dependent on multiple factors. In HeLa and AS-30D tumor cells, glycolysis was regulated predominantly by the hexokinase enzyme, which is feedback inhibited by large concentrations of G6P (Marin-Herandez et al., 2006). Recently, it was found that Glut1 and hexokinase II genes are overexpressed by glucose deprivation and hypoxia (Natsuizaka et al., 2007). It has also been illustrated that almost 50% of the hexokinase activity in rat hepatoma cells is attributed to mitochondrial hexokinase (Arora and Pedersen, 1988; Bustamante and Pedersen, 1977). Further, studies on various tumor cells indicate that the phosphorylating activity of mitochondrial hexokinase is the limiting step compared to the expression levels of Glut1 and hexokinase II enzymes (Aloj et al., 1999). It is possible that the combined effect of hexokinase II expression, phosphorylating activity and availability of ATP is higher in low glucose medium than high glucose medium, leading to a higher glucose uptake in low glucose medium.

The glycolytic pathway is a major source of both energy and precursor metabolites for biosynthesis of nucleic acids, fatty acids and other macromolecules in tumor cells (Mathupala et al., 2006). We observed that the glycolytic rate was higher for the low glucose medium compared to the high glucose medium. Moreover, for glucose-free medium, the glycolytic flux was observed to be quite low. In comparison to glycolysis, the malate to pyruvate glutaminolytic flux, TCA cycle flux and proline to glutamate flux were relatively high in the glucose-free medium (Fig. 6). These alterations initially compensated for the energy production required to maintain cell growth and proliferation (Fig. 1) (Weber et al., 2002). However, these adaptations could not be sustained (Fig. 9C), and by day 3 and onward the cell number in glucose-free medium was significantly lower than in media containing glucose (Fig. 1), further emphasizing the importance of glycolysis in tumor cell proliferation.

HepG2-C3A cells thus show distinct differences from primary hepatocytes in terms of energy metabolism and urea production. To enhance the application of the HepG2-C3A cells in drug testing and bioartificial liver applications, it is important to be able to restore primary hepatocyte

characteristics such as urea cycle activity, as demonstrated already in HepG2 cells by transfection with cDNA encoding urea cycle enzymes (Mavri-Damelin et al., 2007). The importance of the glycolytic pathway in growth and energy metabolism of HepG2-C3A cells has also been illustrated in this study. It has been shown recently that silencing the phosphofructokinase enzyme that catalyzes the conversion of F6P to F16BP induces cell cycle delay and inhibits growth in HeLa cells (Calvo et al., 2006). It has also been demonstrated that hexokinase inhibition restricts tumor growth in colon cancer cells (Fan and WX, 2008; Peng et al., 2008). More recently, 3-bromopyruvate was employed to deplete ATP resources and thereby eradicate advanced tumors (Ko et al., 2004; Pereira de silva et al., 2009). Thus, glycolytic enzymes target cell viability and proliferation, and are effective targets for tumor therapy.

We gratefully acknowledge the financial support from the NSF QSB CBET program (BES-0424968), NSF Metabolic Engineering (BES-0519563), and USEPA-funded Environmental Bioinformatics and Computational Toxicology Center (GAD R 832721-010). We thank Dr. Kyongbum Lee for providing the standard Gibbs free energy data. We also thank Lily Cheung Chang for her technical assistance.

References

Allen JW, Hassanein T, Bhatia SN. 2001. Advances in bioartificial liver devices. Hepatology 34(3):447–455.

Aloj L, Caraco C, Jagoda E, Eckelman WC, Neumann RD. 1999. Glut-1 and hexokinase expression: Relationship with 2-fluoro-2-deoxy-D-glucose uptake in A431 and T47D cells in culture. Cancer Res 59(18):4709–4714.

Arora KK, Pedersen PL. 1988. Functional significance of mitochondrial bound hexokinase in tumor cell metabolism. Evidence for preferential phosphorylation of glucose by intramitochondrially generated ATP. J Biol Chem 263(33):17422–17428.

Barthel A, Schmoll D. 2003. Novel concepts in insulin regulation of hepatic gluconeogenesis. Am J Physiol Endocrinol Metab 285(4):E685–E692.

Bustamante E, Pedersen PL. 1977. High aerobic glycolysis of rat hepatoma cells in culture: Role of mitochondrial hexokinase. Proc Natl Acad Sci USA 74(9):3735–3739.

Calvo MN, Bartrons R, Castano E, Perales JC, Navarro-Sabate A, Manzano A. 2006. PFKFB3 gene silencing decreases glycolysis, induces cell-cycle delay and inhibits anchorage-independent growth in HeLa cells. FEBS Lett 580(13):3308–3314.

Chan C, Berthiaume F, Washizu J, Toner M, Yarmush M. 2002. Metabolic pre-conditioning of cultured cells in physiological levels of insulin: Generating resistance to the lipid-accumulating effects of plasma in hepatocytes. Biotechnol Bioeng 78(7):753–760.

Chan C, Berthiaume F, Lee K, Yarmush ML. 2003a. Metabolic flux analysis of cultured hepatocytes exposed to plasma. Biotechnol Bioeng 81(1):33–49.

Chan C, Berthiaume F, Lee K, Yarmush ML. 2003b. Metabolic flux analysis of hepatocyte function in hormone- and amino acid-supplemented plasma. Metab Eng 5(1):1–15.

Colowick SP. 1961. Review: The status of Warburg's theory of glycolysis and respiration in tumors. Q Rev Biol 36(4):273–276.

DeBerardinis RJ, Mancuso A, Daikhin E, Nissim I, Yudkoff M, Wehrli S, Thompson CB. 2007. Beyond aerobic glycolysis: Transformed cells can engage in glutamine metabolism that exceeds the requirement for protein and nucleotide synthesis. Proc Natl Acad Sci 104(49):19345–19350.

Fan Y, WX Z. 2008. Hacking hexokinase halts tumor growth. Cancer Biol Ther 7(7):1136–1138.

Javitt NB. 1990. Hep G2 cells as a resource for metabolic studies: Lipoprotein, cholesterol, and bile acids. FASEB J 4(2):161–168.

Kanehisa M, Goto S. 2000. KEGG: Kyoto encyclopedia of genes and genomes. Nucl Acids Res 28(1):27–30.

Klamt S, Stelling J, Ginkel M, Gilles ED. 2003. FluxAnalyzer: Exploring structure, pathways, and flux distributions in metabolic networks on interactive flux maps. Bioinformatics 19(2):261–269.

Ko YH, Smith BL, Wang Y, Pomper MG, Rini DA, Torbenson MS, Hullihen J, Pedersen PL. 2004. Advanced cancers: Eradication in all cases using 3-bromopyruvate therapy to deplete ATP. Biochem Biophys Res Commun 324(1):269–275.

Krebs HA, Henseleit K. 1932. Untersuchungen uber die harnstoffbildung im tierkorper. Zschr Physiol Chem 210(33):33–66.

Lee K, Berthiaume F, Stephanopoulos GN, Yarmush ML. 2003. Profiling of dynamic changes in hypermetabolic livers. Biotechnol Bioeng 83(4):400–415.

Llaneras F, Picó J. 2007a. An interval approach for dealing with flux distributions and elementary modes activity patterns. J Theor Biol 246(2):390–408.

Llaneras F, Picó J. 2007b. A procedure for the estimation over time of metabolic fluxes in scenarios where measurements are uncertain and/or insufficient. BMC Bioinformatics 8(1):421.

Lopez-Rios F, Sanchez-Arago M, Garcia-Garcia E, Ortega AD, Berrendero JR, Pozo-Rodriguez F, Lopez-Encuentra A, Ballestin C, Cuezva JM. 2007. Loss of the mitochondrial bioenergetic capacity underlies the glucose avidity of carcinomas. Cancer Res 67(19):9013–9017.

Marin-Herandez A, Rodriguez E, Sara Vital G, Paola A, Flores-Rodriguez FL, Macias-Silva M, Sosa-Garrocho M, Moreno-Sanchez R. 2006. Determining and understanding the control of glycolysis in fast-growth tumor cells: Flux control by an over-expressed but strongly product-inhibited hexokinase. FEBS J 273:1975–1988.

Mathupala SP, Ko YH, Pedersen PL. 2006. Hexokinase II: Cancer's double-edged sword acting as both facilitator and gatekeeper of malignancy when bound to mitochondria. Oncogene 25(34):4777–4786.

Mavri-Damelin D, Eaton S, Damelin LH, Rees M, Hodgson HJF, Selden C. 2007. Ornithine transcarbamylase and arginase I deficiency are responsible for diminished urea cycle function in the human hepatoblastoma cell line HepG2. Int J Biochem Cell Biol 39(3):555–564.

Mavri-Damelin D, Damelin LH, Eaton S, Rees M, Selden C, Hodgson HJF. 2008. Cells for bioartificial liver devices: The human hepatoma-derived cell line C3A produces urea but does not detoxify ammonia. Biotechnol Bioeng 99(3):644–651.

Mavrovouniotis ML. 1991. Estimation of standard Gibbs energy changes of biotransformations. J Biol Chem 266(22):14440–14445.

Mazurek S, Eigenbrodt E, Failing K, Steinberg P. 1999. Alterations in the glycolytic and glutaminolytic pathways after malignant transformation of rat liver oval cells. J Cell Physiol 181(1):136–146.

Moreadith RW, Lehninger AL. 1984. The pathways of glutamate and glutamine oxidation by tumor cell mitochondria. Role of mitochondrial NAD(P)+-dependent malic enzyme. J Biol Chem 259(10):6215–6221.

Moreno-Sanchez R, Rodriguez-Enriquez S, Marin-Herandez A, Saavedra E. 2007. Energy metabolism in tumor cells. FEBS J 274:1393–1418.

Natsuizaka M, Ozasa M, Darmanin S, Miyamoto M, Kondo S, Kamada S, Shindoh M, Higashino F, Suhara W, Koide H, Aita K, Nakagawa K, Kondo T, Asaka M, Okada F, Kobayashi M. 2007. Synergistic up-regulation of Hexokinase-2, glucose transporters and angiogenic factors in pancreatic cancer cells by glucose deprivation and hypoxia. Exp Cell Res 313(15):3337–3348.???

Nielsen J. 1998. Metabolic engineering: Techniques for analysis of targets for genetic manipulations. Biotechnol Bioeng 58(2–3):125–132.

Nolan RP, Fenley AP, Lee K. 2006. Identification of distributed metabolic objectives in the hypermetabolic liver by flux and energy balance analysis. Metab Eng 8(1):30–45.

Park J-K, Lee D-H. 2005. Bioartificial liver systems: Current status and future perspective. J Biosci Bioeng 99(4):311–319.

Pedersen PL. 2007. Warburg, me and Hexokinase 2: Multiple discoveries of key molecular events underlying one of cancers' most common phenotypes, the ''Warburg Effect'', i.e., elevated glycolysis in the presence of oxygen. J Bioenerg Biomembr 39(3):211–222.

Pedersen PL, Mathupala S, Rempel A, Geschwind JF, Ko YH. 2002. Mitochondrial bound type II hexokinase: A key player in the growth and survival of many cancers and an ideal prospect for therapeutic intervention. Biochim Biophys Acta 1555(1–3):14–20.

Peng Q, Zhou Q, Zhou J, Zhong D, Pan F, Liang H. 2008. Stable RNA interference of hexokinase II gene inhibits human colon cancer LoVo cell growth in vitro and in vivo. Cancer Biol Therapy 7(7):1128–1135.

Pereira da silva AP, El-bacha T, Kyaw N, Dos santos RS, Da-silva WS, Almeida FCL, Da poian AT, Galina A. 2009. Inhibition of energy-producing pathways of HepG2 cells by 3-bromopyruvate1. Biochem J 417(3):717–726.

Plant N. 2004. Strategies for using in vitro screens in drug metabolism. Drug Discov Today 9(7):328–336.

Porat N, Apicella MA, Blake MS. 1995. A lipooligosaccharide-binding site on HepG2 cells similar to the gonococcal opacity-associated surface protein Opa. Infect Immun 63(6):2164–2172.

Ranheim T, Kulseth MA, Berge KE, Leren TP. 2006. Model system for phenotypic characterization of sequence variations in the LDL receptor gene. Clin Chem 52(8):1469–1479.

Roth CM, Kohen RL, Walton SP, Yarmush ML. 2001. Coupling of inflammatory cytokine signaling pathways probed by measurements of extracellular acidification rate. Biophys Chem 89(1):1–12.

Schuster S, Fell DA, Dandekar T. 2000. A general definition of metabolic pathways useful for systematic organization and analysis of complex metabolic networks. Nature Biotechnol 18:326–332.

Schuster S, Hilgetag JH, Woods JH, Fell DA. 2002. Reaction routes in biochemical reaction systems: Algebraic properties, validated calculation procedure and example from nucleotide metabolism. J Math Biol 45(2):153–181.

Srivastava S, Chan C. 2008. Application of metabolic flux analysis to identify the mechanisms of free fatty acid toxicity to human hepatoma cell line. Biotechnol Bioeng 99(2):399–410.

Stephanopoulos GN, Aristidou AA, Nielsen J. 1998. Metabolic engineering: Principles and methodologies. San Deigo: Academic Press.

Takanaga H, Chaudhuri B, Frommer WB. 2008. GLUT1 and GLUT9 as major contributors to glucose influx in HepG2 cells identified by a high sensitivity intramolecular FRET glucose sensor. Biochim Biophys Acta 1778(4):1091–1099.

Tilles AW, Berthiaume F, Yarmush ML, Tompkins RG, Toner M. 2002. Bioengineering of liver assist devices. J Hepatobiliary Pancreat Surg 9(6):686–696.

Varma A, Palsson BO. 1994. Metabolic flux balancing: Basic concepts, scientific and practical use. Nat Biotechnol 12(10):994–998.

Warburg O. 1956. On the origin of cancer cells. Science 123(3191):309–314.

Weber K, Ridderskamp D, Alfert M, Hoyer S, Wiesner RJ. 2002. Cultivation in glucose-deprived medium stimulates mitochondrial biogenesis and oxidative metabolism in HepG2 hepatoma cells. Biol Chem 383(2): 283–290.

Wiback SJ, Mahadevan R, Palsson BO. 2004. Using metabolic flux data to further constrain the metabolic solution space and predict internal flux patterns: The *Escherichia coli* spectrum. Biotechnol Bioeng 86(3):317–331.

Wilkening S, Stahl F, Bader A. 2003. Comparison of primary human hepatocytes and hepatoma cell line HepG2 with regard to their biotransformation properties. Drug Metab Dispos 31(8):1035–1042.

Wise DR, DeBerardinis RJ, Mancuso A, Sayed N, Zhang X-Y, Pfeiffer HK, Nissim I, Daikhin E, Yudkoff M, McMahon SB, Thompson CB. 2008. Myc regulates a transcriptional program that stimulates mitochondrial glutaminolysis and leads to glutamine addiction. Proc Natl Acad Sci 105(48):18782–18787.

Yang H, Roth CM, Ierapetritou MG. 2010. Analysis of amino acid supplementation effects on hepatocyte cultures using flux balance analysis. Submitted.